Monthly Notices of the ROYAL ASTRONOMICAL SOCIETY

MNRAS **526,** 456–472 (2023) https://doi.org/10.1093/mnras/stad2702
Advance Access publication 2023 September 07

Recurring outbursts of the supernova impostor AT 2016blu in NGC 4559

Mojgan Aghakhanloo [1]★ Nathan Smith [1] Peter Milne,[1] Jennifer E. Andrews,[2] Schuyler D. Van Dyk [3] Alexei V. Filippenko,[4] Jacob E. Jencson,[5] Ryan M. Lau,[6] David J. Sand,[1] Samuel Wyatt[7] and WeiKang Zheng[4]

[1]*Steward Observatory, University of Arizona, 933 N. Cherry Avenue, Tucson, AZ 85721, USA*
[2]*Gemini Observatory, 670 N. Aohoku Place, Hilo, HI 96720, USA*
[3]*Caltech/IPAC, Mailcode 100-22, Pasadena, CA 91125, USA*
[4]*Department of Astronomy, University of California, Berkeley, CA 94720-3411, USA*
[5]*Department of Physics and Astronomy, The Johns Hopkins University, Baltimore, MD 21218, USA*
[6]*NSF's NOIRLab, 950 N. Cherry Avenue, Tucson, AZ 85719, USA*
[7]*Department of Physics, University of Washington, Seattle, WA 98195, USA*

Accepted 2023 September 1. Received 2023 August 28; in original form 2022 December 19

ABSTRACT

We present the first photometric analysis of the supernova (SN) impostor AT 2016blu in NGC 4559. This transient was discovered by the Lick Observatory Supernova Search in 2012 and has continued its outbursts since then. Optical and infrared photometry of AT 2016blu reveals at least 19 outbursts in 2012–2022. Similar photometry from 1999 to 2009 shows no outbursts, indicating that the star was relatively stable in the decade before discovery. Archival *Hubble Space Telescope* observations suggest that the progenitor had a minimum initial mass of $M \gtrsim 33$ M$_\odot$ and a luminosity of $L \gtrsim 10^{5.7}$ L$_\odot$. AT 2016blu's outbursts show irregular variability with multiple closely spaced peaks having typical amplitudes of 1–2 mag and durations of 1–4 weeks. While individual outbursts have irregular light curves, concentrations of these peaks recur with a period of $\sim$113 $\pm$ 2 d. Based on this period, we predict upcoming outbursts in 2023 and 2024. AT 2016blu shares similarities with SN 2000ch in NGC 3432, where outbursts may arise from periastron encounters in an eccentric binary containing a luminous blue variable (LBV). We propose that AT 2016blu's outbursts are also driven by interactions that intensify around periastron in an eccentric system. Intrinsic variability of the LBV-like primary star may cause different intensity and duration of binary interaction at each periastron passage. AT 2016blu also resembles the periastron encounters of η Carinae prior to its Great Eruption and the erratic pre-SN eruptions of SN 2009ip. This similarity and the onset of eruptions in the past decade hint that AT 2016blu may also be headed for a catastrophe, making it a target of great interest.

Key words: stars: individual: AT 2016blu – stars: massive – stars: variables: general – galaxies: individual: NGC 4559.

1 INTRODUCTION

'Supernova (SN) impostors' are a class of eruptive transient sources found alongside SNe in modern surveys, although they are generally less luminous than SNe and usually have narrow ($\leq$1000 km s^{-1}) H emission lines (Van Dyk et al. 2000; Smith et al. 2011). SN impostors display a wide variety of peak luminosity and light-curve shape, and are usually associated with non-terminal eruptions of evolved massive stars like luminous blue variables (LBVs), based on comparison with giant eruptions of LBVs like η Carinae and P Cygni where the stars are known to have survived. However, the progenitors and physical causes of SN impostor eruptions may be diverse. In the case of AT 2016blu, the transient source discussed in this paper, the star survived its outbursts (and is therefore a likely SN impostor) because it continued to have multiple additional outbursts up to the present time.

AT 2016blu (also known as NGC 4559OT) was discovered as a new transient source on 2012 January 12 (UTC dates are used throughout this paper) by Kandrashoff et al. (2012) during the course of the Lick Observatory Supernova Search (LOSS; Li et al. 2000; Filippenko et al. 2001) with the 0.76 m Katzman Automatic Imaging Telescope (KAIT). AT 2016blu is located about 71 arcsec west and 103 arcsec south of the centre of the galaxy NGC 4559 (see Fig. 1a), in an H II region known as NGC 4559C (or IC 3550). NGC 4559C is at a distance of 8.91 Mpc ($\pm$0.19 statistical, $\pm$0.29 systematic; McQuinn et al. 2017), with Galactic reddening of $E(B-V) = 0.015$ mag (Schlafly & Finkbeiner 2011). However, Sheehan et al. (2014) suggested that AT 2016blu may not be associated with NGC 4559 itself. Given the spatial location and measured recession velocity, they speculated that AT 2016blu is associated with a nearby faint satellite galaxy SDSS J123551.86+275556.9. Kandrashoff et al. (2012) reported that an early-time optical spectrum of AT 2016blu resembled that of the SN impostor SN 2009ip, leading them to suggest that AT 2016blu's 2012 outburst is most likely the eruption of an LBV. AT 2016blu's spectrum exhibits hydrogen Balmer and He I lines with complex P Cygni profiles. The emission lines have

★ E-mail: aghakhanloo@arizona.edu

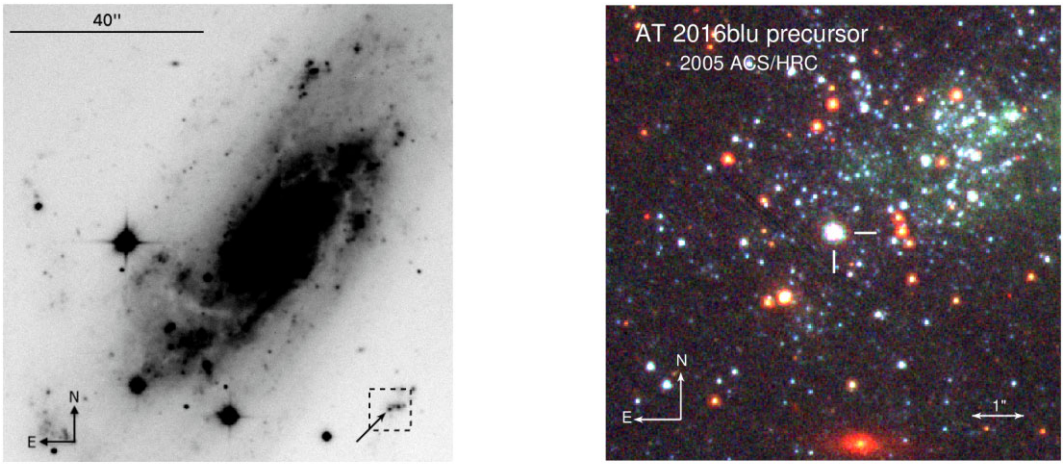

Figure 1. (a) The Kuiper *R*-band image of AT 2016blu obtained on 2018 March 20. The position of AT 2016blu is marked with an arrow. The area inside the dashed square is shown in more detail in panel (b). (b) A colour composite of a portion of the 2005 *HST* ACS/HRC image mosaic (*F*435*W*, blue; *F*555*W*, green; and *F*814*W*, red) showing the AT 2016blu progenitor, indicated by the tick marks. The object was originally identified by Van Dyk et al. (2012).

both narrow and broad components. The narrow lines may arise from slow-moving circumstellar material (CSM), but they might also be contaminated by the emission of an underlying H II region. Unresolved [S II] and [O III] emission lines in the spectrum were attributed to the H II region surrounding AT 2016blu (Sheehan et al. 2014). (Note, on the other hand, that in a spectrum we present later in this paper, the narrow Hα emission persists even though there is little or no contamination from an H II region, judging by the absence of [S II] emission in the same spectrum.) Similarly, ground-based photometric data of AT 2016blu might also be contaminated by continuum emission from the surrounding stellar association.

As we discuss later in this paper, the recurring outbursts of AT 2016blu appear somewhat similar to the series of quasi-periodic outbursts observed in the SN impostor SN 2000ch (Wagner et al. 2004; Pastorello et al. 2010). We recently discussed in detail the long-term light curve of SN 2000ch (Aghakhanloo et al. 2023, hereafter Paper I). SN 2000ch experienced at least 23 known outbursts in 2000–2022. Quasi-periodicities observed in the light curve along with diversity in the properties of outbursts suggest that SN 2000ch's eruptions are caused by interaction around times of periastron in an eccentric binary system. This scenario involves the interplay of two different variability phenomena. One is the intrinsic S Dor-like variability of the LBV (with a time-scale of years), and the other is the observed bright outbursts/eruptions of SN 2000ch (typically lasting a few to several weeks), which are presumably driven by the interaction between the two stars at periastron in the eccentric binary system. (In this work, the terms 'eruption' and 'outburst' are used interchangeably.) Given recent evidence that most LBVs are the products of binary evolution (Smith & Tombleson 2015; Aghakhanloo et al. 2017), it may be unsurprising if the apparent variability of AT 2016blu also arises in an eccentric, interacting binary system, similar to that of SN 2000ch.

The eruptions of AT 2016blu and SN 2000ch have photometric properties similar to the rapid brightening and fading observed in pre-SN eruptions of the well-known SN impostor SN 2009ip (Smith et al. 2010). SN 2009ip provides the most direct link between LBVs and Type IIn SNe (Mauerhan et al. 2013). Recently, Smith et al. (2022) confirmed a terminal core-collapse SN scenario for the dramatic 2012 event in SN 2009ip, because the luminous progenitor star is now gone. Recent evidence also confirms more terminal SN explosions with LBV-like progenitors in other SNe IIn (Brennan et al. 2022; Jencson et al. 2022). Given the similarities to SN 2009ip, one might naturally wonder whether AT 2016blu and SN 2000ch will soon undergo SN explosions, making them targets of great interest.

In this paper, we present the first photometric investigations and period analyses of AT 2016blu. Our main goal is to document major eruptions of AT 2016blu and search for any degree of periodicity similar to that of SN 2000ch. First, in Section 2, we describe the observations. In Section 3, we analyse the major outbursts of AT 2016blu. We discuss AT 2016blu's infrared (IR) variability and study its colour evolution in Section 4. Section 5 investigates the possible periodic variability of AT 2016blu. In Section 6, we analyse *Hubble Space Telescope* (*HST*) data to constrain the mass and luminosity of AT 2016blu's progenitor. Section 7 speculates about the underlying mechanism causing these outbursts, and similarities with SN 2000ch and SN 2009ip. We summarize our conclusions in Section 8.

2 OBSERVATIONS

2.1 Ground-based photometry

We obtained optical photometry of AT 2016blu using the KAIT (Filippenko et al. 2001) at Lick Observatory from 1999 January to the present epoch. The data reduction process is described in Paper I. The unfiltered KAIT photometry of AT 2016blu is summarized in Table A1. Unfiltered KAIT magnitudes are similar to the standard *R* passband (Li et al. 2003). Upper limits derived from KAIT images are available in the online material.

Optical photometry of AT 2016blu was also obtained with the 0.6 m robotic Super-LOTIS (Livermore Optical Transient Imaging System) telescope (Williams et al. 2008) on Kitt Peak, from 2017 May 6 up to the present epoch. Super-LOTIS optical magnitudes and associated uncertainties are given in Table A2. Fig. 2 shows the multiband light curve of AT 2016blu observed by Super-LOTIS. In addition, AT 2016blu was observed using the MONT4K CCD imager on the 61 inch Kuiper telescope on Mt. Bigelow, Arizona; the Kuiper photometry is presented in Table A3.

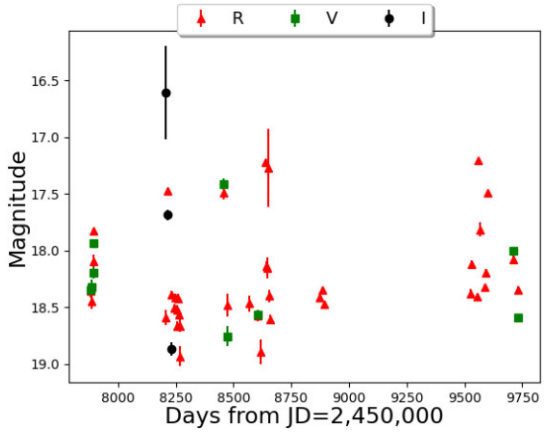

Figure 2. The light curve of AT 2016blu using Super-LOTIS photometry. See Table A2.

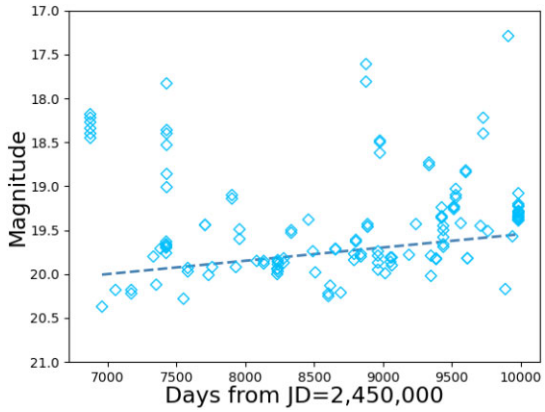

Figure 3. *Gaia* light curve of AT 2016blu. The blue dashed line represents the linear regression fit to the data with magnitudes fainter than 19.3. The fit indicates that the baseline magnitude of the source is increasing by ∼0.5 mag over a span of ∼8 yr.

AT 2016blu was detected by the *Gaia* space telescope (Gaia Collaboration 2016). *Gaia* Photometric Science Alerts system (Hodgkin et al. 2021) reports sources that show significant brightness changes. Gaia16ada is the first SN impostor eruption reported by *Gaia*, and its position coincides with that of AT 2016blu. Fig. 3 shows the *Gaia* light curve of AT 2016blu. The blue dashed line represents the linear regression fit to the base magnitude (>19.3 mag), indicating an increase of ∼0.5 mag in the base magnitude over a period of ∼8 yr. *Gaia G*-band photometry of Gaia16ada is available in the *Gaia* Science Alerts system.[1]

We also retrieved available photometry of AT 2016blu from the Zwicky Transient Facility (ZTF; Bellm et al. 2019) public surveys. ZTF data are available online.[2] We collect the sources within 1 arcsec of the position of AT 2016blu from ZTF Data Release 16. Data from the original Palomar Transient Factory (PTF; Law et al. 2009) are not used because the coordinates are several arcseconds off. We suspect that the source in the PTF photometry is dominated by light from the nearby stellar association, not the transient.

AT 2016blu was observed by the Asteroid Terrestrial-impact Last Alert System (ATLAS) project (Tonry et al. 2018). ATLAS data are available in the ATLAS Forced Photometry server.[3] Data with poor quality and large error bars are excluded from ZTF and ATLAS data (see Paper I for more details). We should note that because AT 2016blu is buried in an H II region and a stellar association, we used ATLAS forced photometry on the difference images instead of forced photometry on the target images.

We include various discovery data from the 'Bright Supernovae' website[4] maintained by David W. Bishop. This website compiles data from amateur astronomers whose observations are collected in various types of filters (or unfiltered). Later, in Section 3, we only use observations that are reported as discovery. The Discovery report specifies that AT 2016blu was bright at the time and there should be outburst activity around the reported time. However, since AT 2016blu exhibits multiple narrow peaks (see Section 3 for more details), photometry gathered on the Bright Supernovae website might correspond to the fluctuations before or after the main event. If these discoveries are not supplemented with more data, the precise time of the outburst remains uncertain.

IR data were obtained with the *Spitzer Space Telescope* (*Spitzer*), as described below.

2.2 *HST* observations

The site of AT 2016blu was serendipitously observed on three occasions with *HST* in the decade prior to the 2012 outburst: on 2001 May 25 (GO-9073, PI: J. Bregman) with the Wide-Field Planetary Camera 2 (WFPC2) in bands *F*450*W*, *F*555*W*, and *F*814*W*, each with 2000 s exposure time; on 2005 March 8 (GO-10214, PI: R. Soria) with the Advanced Camera for Surveys (ACS)/High Resolution Channel (HRC) in *F*435*W*, *F*555*W*, *F*814*W*, *F*502*N*, and *F*658*N*, each with 2400 s exposure time; and on 2005 March 9 (GO-10214) with the ACS/Wide Field Channel in *F*606*W* (5920 s) and *F*550*M* (5581 s). All of these publicly available archival data were obtained from the Mikulski Archive for Space Telescopes portal. We first processed the individual pipeline-processed exposure frames with ASTRODRIZZLE (STSCI Development Team 2012), before running them through the *HST*-optimized photometry routine Dolphot (Dolphin 2016); a major advantage of undertaking the former is the identification and masking of cosmic ray hits in the frames, removing the effect of these artefacts on the Dolphot aperture correction step.

Our analysis here was greatly simplified, since Van Dyk et al. (2012) had already located the progenitor in these *HST* data, which we show in Fig. 1(b). The object is in the same complex region of the galaxy as the optical counterpart of the ultraluminous X-ray source X7 studied by Soria et al. (2005), although ∼12 arcsec to the south-east (cf. their fig. 2). It is striking that the AT 2016blu progenitor is one of the brightest objects in the field in these pre-outburst images. Interestingly, Soria et al. (2005) estimate that the evolved stars in the surrounding region (mostly blue and red supergiants) have luminosities corresponding to initial masses of 10–15 $M_{\odot}$, implying ages of ∼20 Myr for the population. The field of view in Fig. 1(b) includes an 8 arcsec × 8 arcsec region, showing the stellar population within a radius of 175 pc. *HST* raw magnitudes are given in Table A4. In Section 6, we use the *HST* data to constrain properties of the AT 2016blu progenitor.

[1] http://gsaweb.ast.cam.ac.uk/alerts/home
[2] https://irsa.ipac.caltech.edu/Missions/ztf.html
[3] https://fallingstar-data.com/forcedphot/
[4] https://www.rochesterastronomy.org/supernova.html

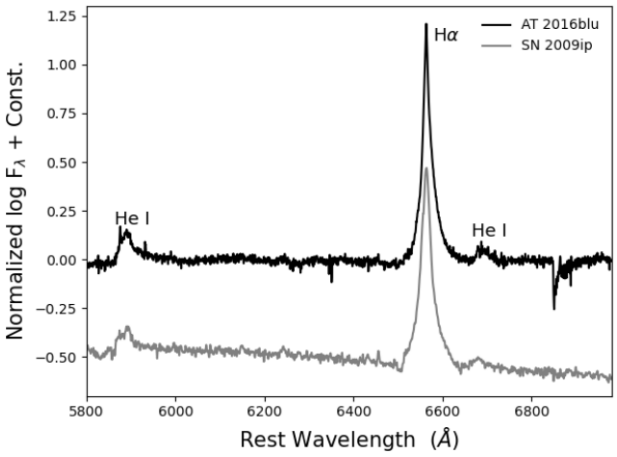

Figure 4. MMT Blue Channel spectrum of AT 2016blu obtained on 2019 June 4, coincident in time with AT 2016blu's 11th outburst (see Fig. 6i). Hα does not show a P Cygni profile and its Lorentzian FWHM is $\sim$415 km s^{-1}; correcting by quadrature for the instrumental resolution of $\sim$80 km s^{-1} with the 1200 lines mm^{-1} grating, the FWHM is $\sim$410 km s^{-1}. The He I lines at 5876 and 6680 Å are also visible. The day 25 spectrum of SN 2009ip from Smith et al. (2010) is shown for comparison.

2.3 Infrared photometry

The site of AT 2016blu was also imaged by the *Spitzer* at wavelengths of 3.6 and 4.5 μm (*Spitzer*/IRAC (Infrared Array Camera) Bands 1 and 2). To measure the brightness of the object, we used a 2 native-pixel (radius) aperture of 2.4 arcsec. We used a background annulus ranging from 2 to 6 native pixels (2.4–7.2 arcsec) to measure and subtract the background emission. We applied aperture correction factors of 1.2132 and 1.2322 for the *Ch*1 and *Ch*2 filters, respectively. These values are consistent with the correction factors recommended in the *Spitzer*/IRAC manual for the chosen aperture and background annulus radii. The *Spitzer* photometry can be found in Table A5.

The angular resolution of the *Spitzer* imaging is significantly lower than that of the *HST* observations, and the *Spitzer* photometry therefore necessarily includes contamination from some of the neighbouring stars seen in Fig. 1(b). We are mostly interested in changes in the IR excess emission that may be associated with outbursts in the past decade. Therefore, we also subtracted a baseline flux corresponding to the epoch in 2004 when the source was at its faintest recorded magnitude in the *Spitzer* bands before the first outburst in 2012, and the differences in magnitudes are discussed below. Similarly, the last column in Table A5 includes the *Ch*1/*Ch*2 colour after subtracting this 2004 baseline flux level.

2.4 Spectroscopy

An optical spectrum of AT 2016blu (Fig. 4) was obtained on 2019 June 4 with the Blue Channel spectrograph on the 6.5 m MMT (Multiple Mirror Telescope) Observatory on Mount Hopkins, Arizona, coincident in time with AT 2016blu's 11th outburst (see Section 3 for more details). It exhibits a very strong, relatively narrow emission line of Hα with a Lorentzian full width at half-maximum intensity (FWHM) of $\sim$410 km s^{-1} (corrected for the instrumental resolution). Weaker emission lines from He I at $\lambda\lambda$5876 and 6680 Å are also visible. In Fig. 4, AT 2016blu's spectrum is compared with that of the 2009 pre-SN outburst of SN 2009ip from Smith et al. (2010). The spectra are very similar, and the $\sim$550 km s^{-1} FWHM of the Hα line in SN 2009ip (Smith et al. 2010) is comparable to that of AT 2016blu reported here. A much more detailed analysis of AT 2016blu's spectral evolution will be discussed in a forthcoming paper.

3 THE LIGHT CURVE

The full light curve of AT 2016blu is shown in Fig. 5; Fig. 5(a) displays the light curve from 1999 to 2009, while Fig. 5(b) shows the light curve from 2012 to 2023 February.

In Fig. 5(a), we see that the host galaxy of AT 2016blu was monitored by KAIT for $\sim$11 yr, with no detections of a source at AT 2016blu's position. Based on these KAIT upper limits, the magnitude of AT 2016blu remained $\sim$19 or fainter. This is fainter than many of the outburst peaks seen in the 2012–2022 decade, and there are KAIT upper limits at times when we may expect an outburst based on the quasi-periodicity found below from the more recent data, indicating that AT 2016blu was not experiencing its repeated eruptions before 2009. This may be important for understanding the origin of AT 2016blu's eruptions, and we return to this fact later. In Fig. 5(a), we also see that the progenitor star detected in *HST* images (discussed below) was safely below the KAIT upper limits around the same time period, consistent with KAIT non-detections of the quiescent progenitor star.

The more recent decade (Fig. 5b) demonstrates much greater activity in AT 2016blu. Super-LOTIS data are in the Johnson–Bessell photometric system. Unfiltered KAIT photometry is roughly similar to the *R* band (Li et al. 2003). ZTF observations are in the ZTF *r* filter, which is close to the SDSS (Sloan Digital Sky Survey) *r* filter; ZTF data are therefore scaled to Johnson–Bessell *R* by applying a shift of -0.18 mag. The *Gaia G* band approximately corresponds to SDSS *g*, and the *o*-band ATLAS filter roughly corresponds to SDSS $r + i$. Data from the Bright Supernovae website are a mixture of various filters (*U*, Clear, and *V*). As we mentioned before, AT 2016blu is also coincident with an H II region, which can lead to flux contamination. Instead of transforming the bands, we adjust fluxes from each data set to approximately match all data sets. The offset values are either estimated based on the flux difference between two data sets when they coincided in time, or they are determined visually to make the base quiescent magnitudes between the two data sets the same. Fig. 5(b) shows the light curve after flux adjustment. All of the offsets indicated in Fig. 5(b) correspond to a shift associated with a base magnitude of $\sim$18.5. Since our goal is to search for periodicity, not derive physical properties, these shifts are merely for clarity of displaying the light curves.

The solid vertical grey bands indicate the time interval each year, from August 26 to October 24, when AT 2016blu is difficult or impossible to observe owing to its position being too close to the Sun in the sky. It is expected that some outbursts fall within these unobservable windows or at a boundary, since the outbursts seem to repeat with a period of less than a year (see Section 5 for more details).

Using our photometric observations, we find that AT 2016blu experienced at least 19 outbursts during the interval 2012–2022. All of AT 2016blu's known outbursts are summarized in Table 1, and light curves for various individual eruptive events are shown in several panels in Fig. 6. We note that AT 2016blu brightened by $\sim$0.8 mag in 2012 May and experienced a dip in 2019 October. However, the data coverage during these times is insufficient to study the detailed evolution of the light curve. We define an outburst as a brightening that is more than $\sim$1 mag, and any clustered observations with multiple peaks are considered part of the same outburst. The

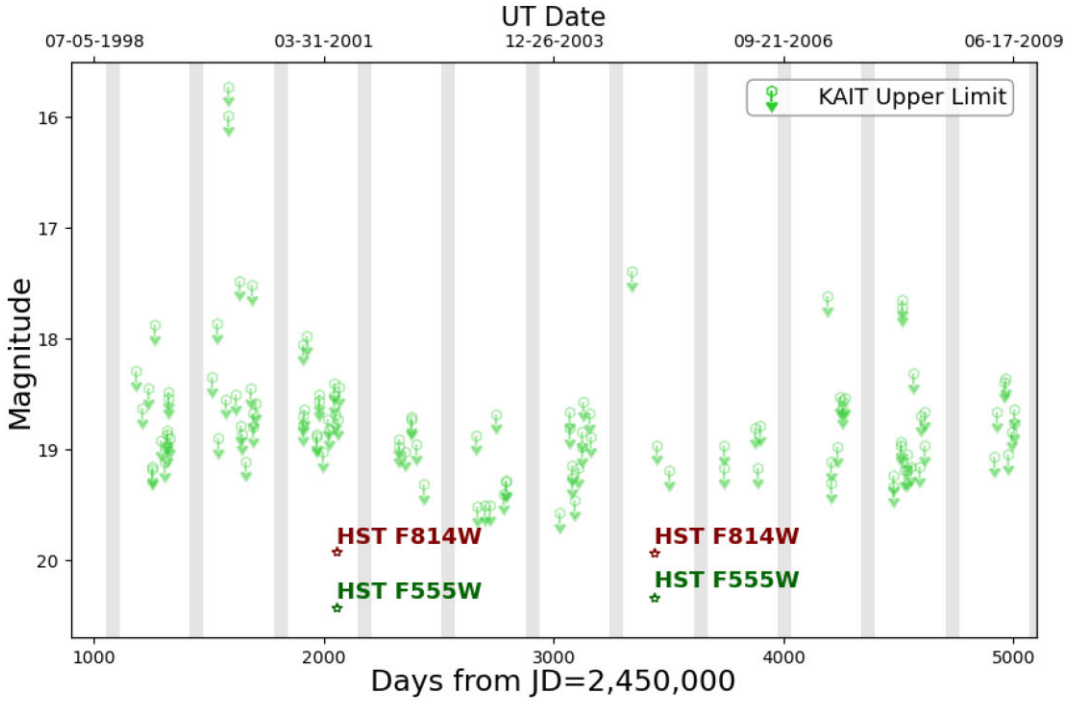

(a)

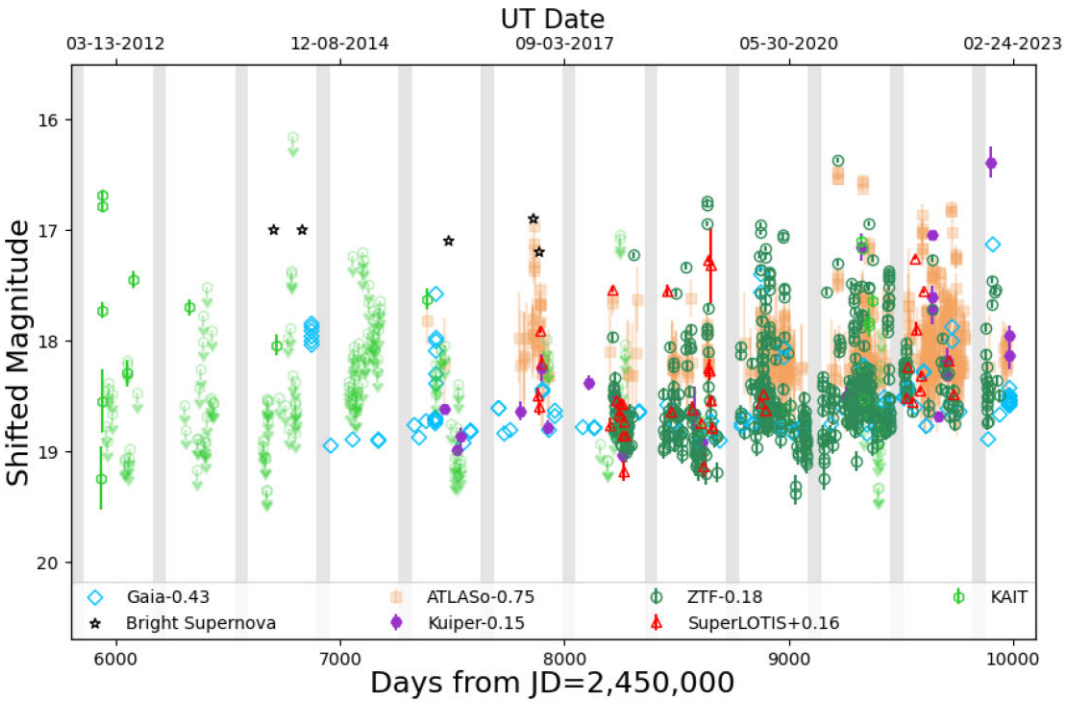

(b)

Figure 5. The observed light curve of AT 2016blu, mostly in *R*, but ATLAS data are in the 'orange' (*o*) filter, *Gaia* data are in the *G* band, and Bright Supernovae website data are in various filters or unfiltered. (a) The light curve from 1999 to 2009, where only KAIT upper limits are available. (b) The light curve from 2012 to 2023 February. The light curve is displayed with flux adjustment for each data set to roughly match them with one another. Vertical grey areas indicate times each year, from August 26 to October 24, when AT 2016blu is difficult to observe owing to its proximity to the Sun in the sky. Photometric observations cover at least 19 outbursts in 2012–2022. See Fig. 6, which zooms-in on individual eruption events.

Table 1. Summary of AT 2016blu's 19 known outbursts from 2012 to 2022.

Outburst #	Peak (JD−2450 000)	Expected outburst time (JD−2450 000)	Approx. amplitude (mag)	Approx. duration (d)	Ref.
1	5938.9	5938.9	2.6	6.0	LOSS/this work
2	6704.2	6729.4	–	–	Itagaki[a]
3	6831.4	6842.3	–	–	Cortini[a] and this work
4	7427.5	7406.9	1.2	45.0	This work
5	7484.4	7519.8	–	–	Arbour[a]
6	7862.2	7858.6	–	–	Itagaki, Arbour,[a] and this work
7	8213.9	8197.3	1.3	>31.1	This work
8	8306.7	8310.2	1.7	35.7	This work
9	8457.0	8423.2	1.4	>31.0	This work
10	8543.8	8536.1	1.7	75.8	This work
11	8636.7	8649.0	2.5	26.3	This work
12	8876.0	8874.8	2.0	84.9	This work
13	8976.8	8987.8	1.9	39.0	This work
14	9217.9	9213.6	2.6	70.9	This work
15	9324.9	9326.5	2.1	96.8	This work
16	9444.6	9439.4	1.5	24.9	This work
17	9560.0	9552.4	1.5	62.7	This work
18	9640.0	9665.3	1.6	42.9	This work
19	9903.0	9891.1	2.5	64.1	This work

[a]https://www.rochesterastronomy.org/sn2012/lbvn4559.html

end of an outburst is also defined based on the quality and sampling of the data, as the outbursts are irregular.

In the following, we describe each event in detail. The designation for each event below corresponds to the date of the peak brightness, represented by a data point with the brightest magnitude inside the 'outburst window'. In some cases, the time of the outburst is unclear either owing to poor data coverage or multiple rapid peaks with similar magnitudes. The designation for these events is instead based on the expected time of the outburst using the detected period (based on a periodogram analysis of the light curve; see Section 5). In each plot, the red dashed line shows the expected time of the outburst, which is derived from $d_{\rm red} = 2455\,938.9 + 113\,n$, while the brown dotted line shows the reference epoch using the second most dominant period in the periodogram, which is 38.5 d. Similar to Paper I, *o*-band ATLAS data are shown in the background, but they are not used to define a period because they are in a different filter and many points are close to the limiting magnitude of that telescope (∼19 mag).

2012 January: Fig. 6(a) shows the first detected outburst of AT 2016blu. On 2012 January 12, the object reached maximum brightness, with $m_R = 16.7$ mag. This event is used as the reference epoch, shown as the red dashed line in Fig. 6 and several figures that follow.

2014 February: K. Itagaki reported an outburst discovery of AT 2016blu on 2014 February. During the time of the reported discovery, no additional optical data were available to study the evolution of the light curve in detail. Fig. 7 shows the mid-IR light curve of AT 2016blu, which confirms the outburst reported by K. Itagaki.

2014 June: In mid-2014, G. Cortini reported the discovery of another outburst of AT 2016blu. Shortly thereafter, the object experienced a slight decline in its brightness (see Fig. 6b). Given our derived period of ∼113 d (see Section 5), the time of the reported discovery is within ∼11 d of an expected event.

2016 January: Fig. 6(c) shows that around 2015 December, AT 2016blu reached an apparent magnitude of 17.6. Soon thereafter in 2016 February, the *Gaia* Photometric Alerts page reported that AT 2016blu reached a maximum brightness of 17.6 mag. During the fourth outburst, AT 2016blu experienced multiple peaks with similar magnitudes. A brighter peak could have been missed if it occurred between these peaks when there was a lack of data. Therefore, the designation for this event is associated with the expected time of the outburst (red dashed line).

2016 April: In mid-2016, R. Arbour reported the discovery of another outburst of AT 2016blu (Arbour 2016). Similar to previous events, the exact time of the fifth outburst is uncertain owing to the lack of optical data. None the less, Fig. 7 shows that this outburst was also captured in mid-IR observations. This source was named AT 2016blu by R. Arbour after the 2016 April outburst, even though it experienced multiple outbursts before 2016. Prior to this event, the source had been referred to as NGC 4559OT.

2017 April: AT 2016blu experienced two bright phases in 2017 April and May reported in the Bright Supernovae webpage. Fig. 6(d) shows that ATLAS data reinforce the first peak brightness, while the secondary peak was covered by both ATLAS and Super-LOTIS.

2018 April: In 2018, AT 2016blu experienced its seventh recorded outburst, when it reached an apparent magnitude of 17.5 (Fig. 6e). The observed peak of the outburst corresponds more closely to a shorter period of 38.5 d (brown dotted line) than to a longer period of ∼113 d (red dashed line). Perhaps the main peak is missed in this case.

2018 July: AT 2016blu experienced its eighth outburst in 2018 July, when it brightened by 1.7 mag, and it reached an apparent magnitude of 17.2 (see Fig. 6f).

2018 December: In December, AT 2016blu brightened again and reached $m_R = 17.6$ mag. The main peak might have been missed because AT 2016blu was difficult to observe prior to this time (Fig. 6g).

2019 March: In 2019, AT 2016blu experienced multiple fluctuations in its apparent magnitude. The 2019 March event shows spikes with similar magnitudes instead of a big spike in its brightness, as illustrated in Fig. 6(h).

2019 June: Fig. 6(i) shows that in 2019, AT 2016blu experienced a sharp brightening by ∼2.5 mag, followed by a secondary peak similar to its previous events. The first peak is more consistent with

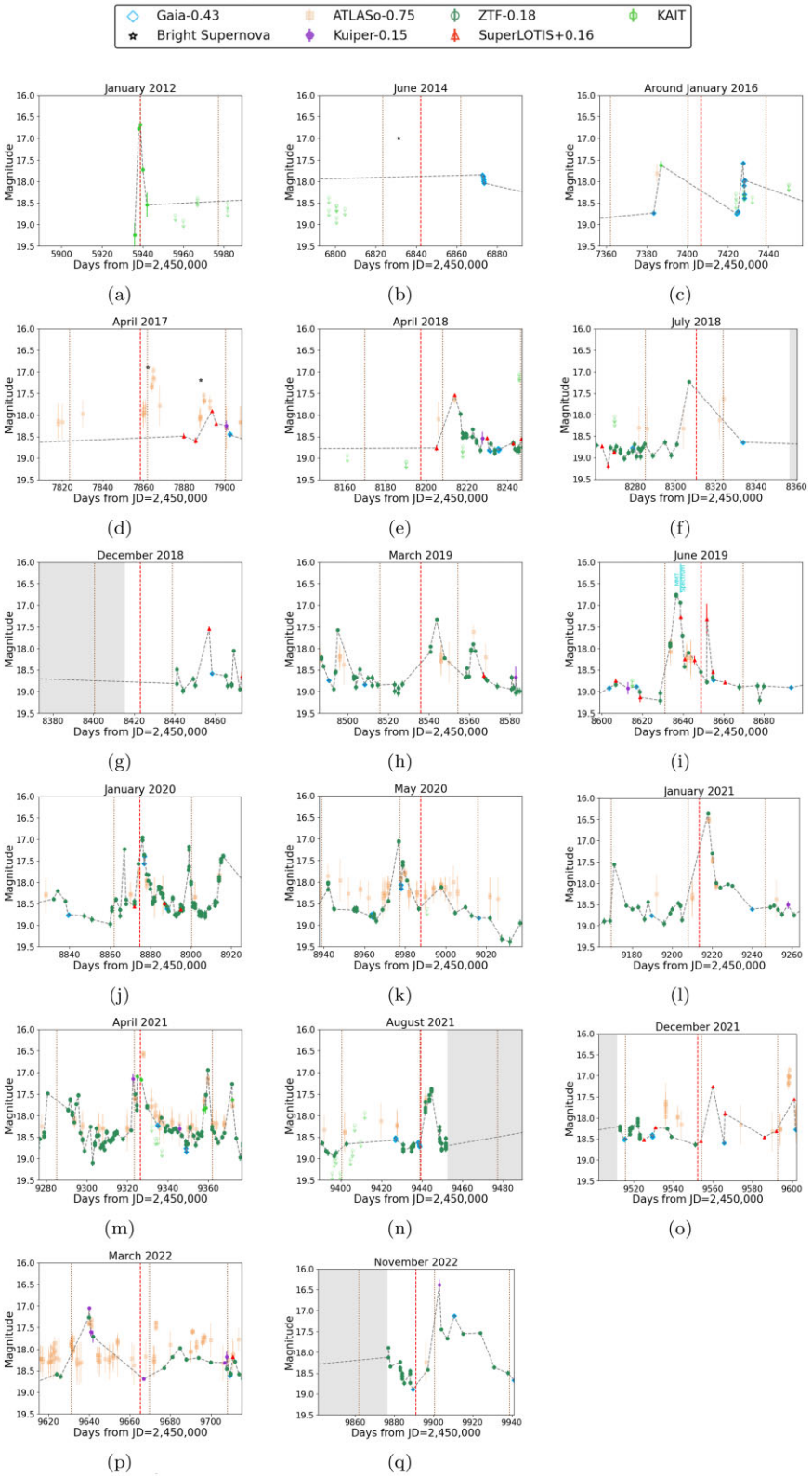

Figure 6. Zoomed-in light curves of AT 2016blu during its multiple outbursts. The data points from all surveys, excluding ATLAS, are connected together with a dashed line. These data points are used to estimate the period. The approximate time of each outburst is given at the top of the frame. The red dashed line shows the reference epoch adopting the most likely period of ∼113 d from the periodogram, tied to the first outburst in 2012 January. On the other hand, the brown dotted line shows the reference epoch using the second most dominant period in the periodogram. Some of the outbursts align better with the smaller period of 38.5 d. Quasi-periodic behaviour is evident relative to the reference epoch.

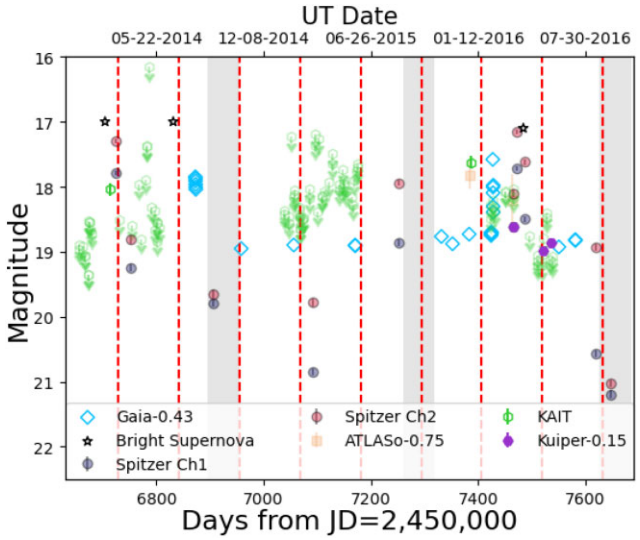

Figure 7. Mid-IR light curve of AT 2016blu obtained with *Spitzer*, which captured two outbursts of AT 2016blu in 2014 and 2016. The *Ch*1 and *Ch*2 *Spitzer* data have a constant baseline flux subtracted; this flux is taken from the minimum observed flux before 2012, which was recorded in 2004 May. (This baseline IR flux may include emission from the quiescent progenitor or its associated stellar population.)

the shorter period, and the second peak is more consistent with the longer period. This suggests that the second dominant peak in the periodogram may be attributed to multiple luminosity spikes occurring in each event. Fig. 4 displays the MMT Blue Channel spectrum of AT 2016blu (1200 lines mm^{-1} grating) obtained on 2019 June 4, coincident in time with AT 2016blu's 11th outburst.

2020 January: AT 2016blu experienced its 12th outburst in early 2020 (see Fig. 6j). The 2020 January event has multiple brightness peaks with approximately similar magnitudes. The middle peak was slightly brighter, $m_R = 17.0$ mag.

2020 May: In 2020 May, AT 2016blu reached an apparent magnitude of 17.0 (see Fig. 6k). The observed peak aligns more with the expected time of the outburst based on the shorter period. The dip in the middle of the two main peaks is reminiscent of the dips seen during some eruptions in SN 2000ch's light curve, for which extinction from new dust formation was a suggested cause (see Paper I for more details). Alternatively, the dips might be artificial if they are the result of the combination of the different bands from different telescopes.

2021 January: Fig. 6(l) shows that in early 2021, AT 2016blu experienced multiple closely spaced peaks of varying brightness, somewhat similar to the 2019 March event. The second peak is brighter, where AT 2016blu brightened by 2.6 mag.

2021 April: Again similar to previous events, AT 2016blu experienced multiple fluctuations with approximately similar magnitudes in mid-2021 (Fig. 6m). Although the peak observed in 2021 May is slightly brighter than the one in April, we designate the peak in April as the main event because it aligns better with the estimated time of outburst. ATLAS data show a spike in 2021 April, consistent with the peak, where AT 2016blu reached $m_R = 17.1$ mag.

2021 August: Later in August, AT 2016blu experienced another outburst right before it became difficult to observe (Fig. 6n). During its 16th outburst, AT 2016blu brightened by 1.5 mag.

2021 December: In late 2021, AT 2016blu reached $m_R = 17.3$ mag. Fig. 6(o) shows that AT 2016blu experienced two more fainter peaks subsequently, and one of them is supported by ATLAS data.

2022 March: Fig. 6(p) shows that in 2022 March, AT 2016blu experienced its 18th outburst, where it brightened again and reached $m_R = 17.0$ mag. The observed peak is more consistent with the shorter period (brown dotted line) rather than the longer period (red dashed line), unless the main peak was missed.

2022 November: In late 2022, AT 2016blu reached $m_R = 16.4$ mag (see Fig. 6q). During this outburst, AT 2016blu brightened by 2.5 mag. Similarly to the previous event, the observed peak is more in agreement with the expected time of the outburst based on the shorter period.

4 WAVELENGTH DEPENDENCE

4.1 Variability in the mid-infrared

As we mentioned in the previous section, AT 2016blu's two outbursts in 2014 and 2016 were also observed by *Spitzer*. Fig. 7 shows the mid-IR and optical light curve of AT 2016blu. These outbursts were also supported by optical observations made by amateur astronomers as discussed in Section 3. An IR source coincident with AT 2016blu was also detected back in 2004 (not shown in Fig. 7; see Table A5), but it is not clear whether AT 2016blu was in outburst or quiescence during that time; moreover, that IR flux may include light from neighbouring stars or the nearby H II region, as discussed below.

Given that the quiescent *Spitzer* flux may be contaminated by some light from the underlying stellar population, and since we are most interested in the change in IR excess emission during outburst, in Fig. 7 we show the *Spitzer* data after subtracting the minimum observed flux before 2012, which was recorded in 2004 May. It is clear that after this subtraction, there is significant excess IR flux that is due to transient emission from eruptions of AT 2016blu. The observed excess IR emission could be due to (1) blackbody radiation from the photosphere of AT 2016blu itself, (2) newly formed dust in material ejected by AT 2016blu, or (3) pre-existing CSM dust ejected previously by AT 2016blu that is heated by the rising luminosity of the outburst. It is possible to determine whether IR emission is caused by dust emission or originates from enhanced radiation from the photosphere via *Spitzer* colours. The colour estimates in Table A5 range from 0.14 to 1.63 mag, which are redder than the expected *Spitzer* colour in these bands for the Rayleigh–Jeans tail of the transient's photosphere. The expected colour for a star with a temperature of higher than 7000 K (see Section 6 for more details regarding the estimated temperature) is 0–0.1 mag or bluer, as shown in fig. 7 of Bonanos et al. (2010). The detection of an IR excess suggests the presence of dust in the vicinity of AT 2016blu. Owing to a lack of sufficient optical observations during the IR peaks, we are unable to determine whether the dust is newly formed or pre-existing.

4.2 Visual-wavelength colour evolution

Fig. 8 shows the colour evolution of AT 2016blu based solely on ZTF data without any magnitude shift. As multiband observations were not taken simultaneously, we interpolate the data set with a larger number of data points (r and g bands), in order to match the sampling size of the smaller data set (i band). This allowed us to approximate the r- and g-band data at the same time as the i-band data. When we interpolate the data, we also need to account for the uncertainty in the measurements. To do this, we assign the magnitude uncertainty of the interpolated data to be the same as the magnitude uncertainty of the closest magnitude in that specific band. In other words, we look for the closest measurement in the same band and use its magnitude uncertainty as the uncertainty for the interpolated

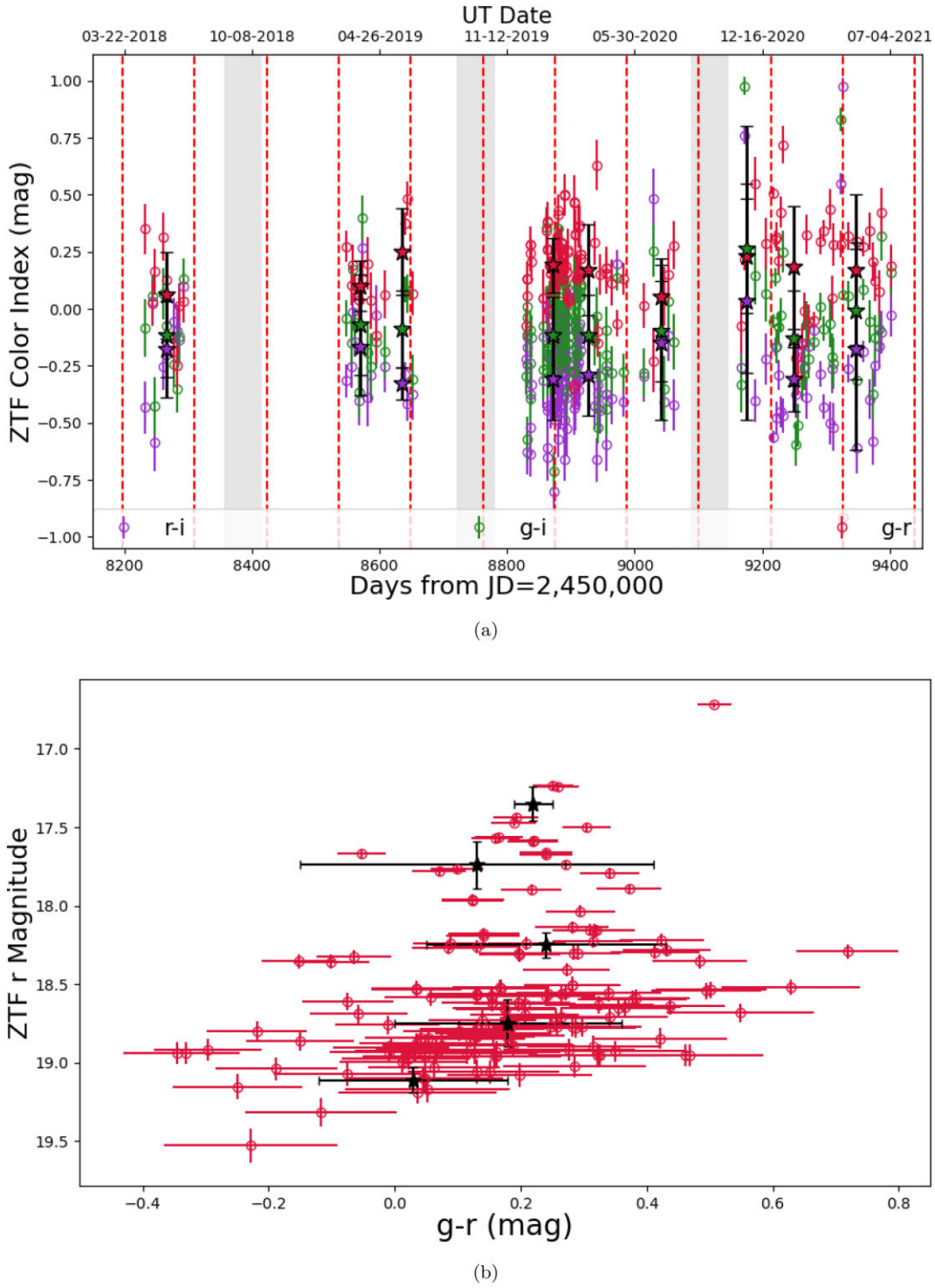

Figure 8. Colour evolution of AT 2016blu using only ZTF Sloan filters, with no magnitude shift. (a) The colour evolution over time in $r - i$ (purple), $g - i$ (green), and $g - r$ (red). The points marked with a star symbol represent the average colour obtained by binning the colour light curve. (b) The ZTF *r*-band magnitude as a function of $g - r$ colour. Black points represent the average colour and *r* magnitude for each magnitude bin. There is no significant evidence of a change in colour over time for AT 2016blu.

data. The colour uncertainty corresponds to the uncertainties in each band added together in quadrature.

Fig. 8(a) shows that the colour of AT 2016blu does not exhibit a consistent pattern with respect to times of outburst, with relatively small colour changes of $\lesssim$0.5 mag in any individual colour. Fig. 8(b) shows *r* magnitude as a function of $g - r$ colour, which is meant to determine whether the colour changes systematically with brightness level. In order to assess whether there is a significant change in colour over time, the data have been grouped into bins of size 0.5 mag (indicated by black points). The difference in colour is smaller

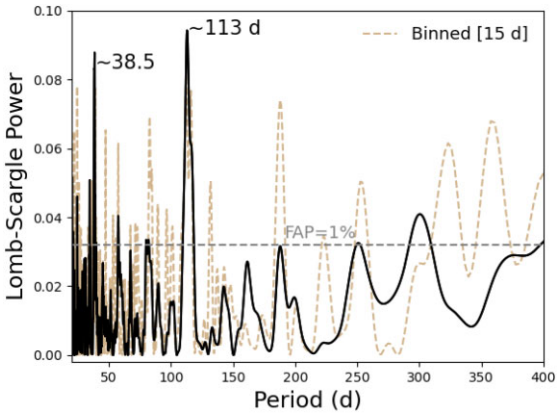

Figure 9. The Lomb–Scargle periodogram of AT 2016blu's light curve using optical photometry data from various facilities spanning from 2012 to 2023 February (excluding upper limits and ATLAS data). We find that the outbursts seem to repeat with a most likely period of 112.9 d. Two smaller peaks with lower amplitudes can also be observed at ∼35 and ∼38 d. These peaks are likely to be associated with multiple spikes occurring either before or after each outburst. The 1 per cent FAP level is indicated by a horizontal dashed line. Additionally, we generated a periodogram of the binned light curve (brown dashed line), which shows a similar optimal period when the bin size is less than ∼15 d. However, larger bin sizes result in a periodogram without a single strong peak because the bright peaks get removed during binning.

than the deviation and the data are therefore in agreement with the same colour over time. Overall, this indicates that any colour shift is small ($\lesssim$0.25 mag) compared to the amplitude range of eruptions (1–2 mag). While traditional LBVs are expected to become much cooler as they brighten, a subset of LBV-like transients, including SN 2009ip's progenitor, SN 2000ch, and M33 MCA-1B, appears to remain hot at its peak brightness level (Smith et al. 2010, 2011, 2020; Paper I).

Next, we investigate the possible presence of periodic behaviour in the light curve of AT 2016blu, utilizing the Lomb–Scargle periodogram. This statistical tool is commonly used for detecting periodic signals in observations that are not evenly spaced. As in the case of SN 2000ch (Paper I), finding periodic behaviour could give a hint of the underlying mechanism that triggers these outbursts.

5 SEARCH FOR PERIODICITY

In this section, we use the methodology presented in Paper I to identify possible periodic behaviour in the light curve of AT 2016blu. First, we use a Lomb–Scargle periodogram, and then we fold the light curve to analyse its period variation.

Fig. 9 shows the Lomb–Scargle periodogram (Lomb 1976; Scargle 1982; VanderPlas 2018) of AT 2016blu's light curve, for possible periods between 20 and 400 d. We find that AT 2016blu's eruptive outbursts repeat with a best period of 112.9 d. The false-alarm probability (FAP) of this peak is very small, of the order of 10^{-14}, meaning that this peak is statistically significant. The horizontal dashed line in Fig. 9 shows the 1 per cent FAP level. Based on the duration of the outbursts, the uncertainty in the period should be ∼2 d.

Two smaller amplitude peaks can also be seen around 35 and 38 d. As we discussed in Section 3, AT 2016blu experienced multiple fluctuations in its apparent magnitude. We find the separation between closely spaced peaks to be 20–50 d, suggesting that the two low-period peaks in the periodogram might be due to multiple rapid spikes in luminosity. In Section 3, we demonstrated that some of the luminosity peaks are more closely aligned with the shorter period of 38.5 d (see dashed brown lines in Fig. 6).

We conduct additional analyses by binning the light curve using various bin sizes and performing a search on the binned light curve to verify the robustness of our primary findings. Our results show that bin sizes less than ∼15 d result in a similar optimal period as our primary analysis. However, larger bin sizes do not reveal a single strong peak in the periodogram. This outcome is expected because a bin size of more than 15 d becomes larger than the peak duration of most of the outbursts, and therefore begins to dilute or erase the signal.

We then carry out the period analysis by folding the light curve with the detected period of ∼113 d. Fig. 10 shows the folded light curve of AT 2016blu, which is like a two-dimensional observed minus calculated plot. All the data are time-shifted by $n \times 113$ d (n is from 0 to 26). Cycles with poor data coverage are excluded, and dashed lines show the months (August–October) when AT 2016blu was difficult to observe. Black lines indicate the evolution of the variable star during the 19 major outbursts. The red vertical dashed line shows the reference epoch, which is derived from the first outburst in 2012 January. Similar to SN 2000ch's light curve (Paper I), AT 2016blu's light curve exhibits quasi-periodic variation, but AT 2016blu's outbursts are more irregular. While many individual outbursts align well with the predicted time, some – especially cases where there are multiple outbursts – seem to straddle the expected time or are offset slightly. Several outbursts may have been missed for different reasons: (1) outbursts coincident in time with when AT 2016blu could not be observed owing to its position relative to the Sun, and (2) poor data coverage at the time of the outburst. It is unlikely that the outbursts look dimmer owing to dust formation close to the star. If faint points were intrinsically bright but appeared faint because of extinction, they would also be systematically reddened and would therefore be located towards the lower right in Fig. 8(b), which is currently empty.

Fig. 11 displays the full light curve again with calculated times of events using a period of ∼113 d (red vertical lines). Fig. 11(a) shows the light curve over a period of ∼11 yr where only upper limits are available. Some upper limits overlap with the predicted times of the outbursts. This implies that AT 2016blu did not experience outbursts prior to 2009. However, since there is a lack of data between mid-2009 and 2012 (the KAIT data were lost, unfortunately, because two storage disks malfunctioned), we cannot determine whether the outburst began before 2012 or the 2012 event was the first outburst. Fig. 11(b) shows the light curve from 2012, and the period of ∼113 d matches most of the outbursts, considering that some of the main brightness peaks might be missed as we described above. This suggests that the period is not changing significantly over time. There are KAIT upper limits that overlap with some predicted times of the outbursts after 2012. However, it is challenging to determine whether AT 2016blu was undergoing an outburst during those times because brightness peaks are narrow and may occur just before or after the expected time.

Fig. 12 displays the phase diagram of AT 2016blu, where all the cycles are folded on top of each other. The phase diagram shows two complete cycles, and to better see the behaviour of AT 2016blu, a folded light curve is binned. Black points in Fig. 12 indicate average magnitudes after binning the folded light curve. AT 2016blu seems to get brighter around phase zero, which is set using the first outburst in 2012 January.

Above, we demonstrated that AT 2016blu experienced multiple outbursts over the past ∼11 yr. Using the Lomb–Scargle peri-

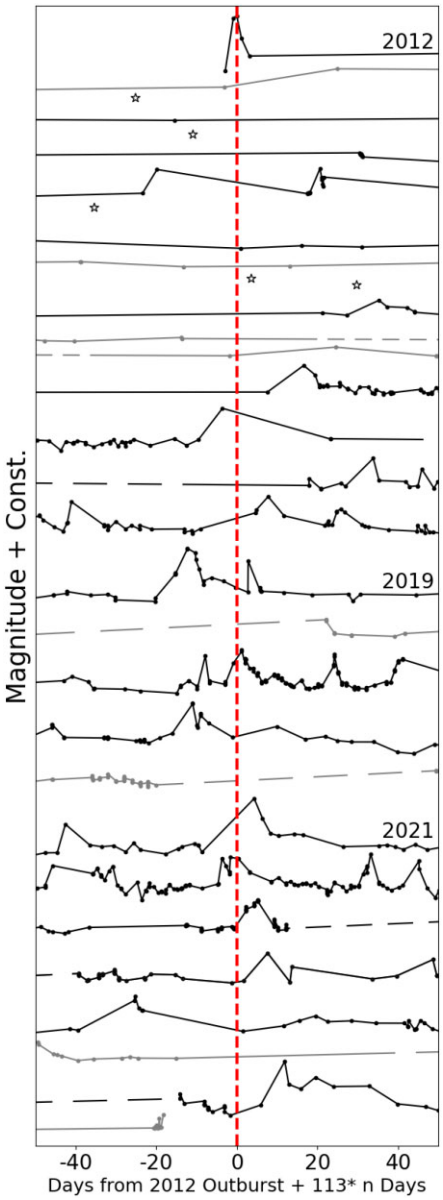

Figure 10. Folded light curve of AT 2016blu using a period of ∼113 d. ATLAS data and points with upper limits are not shown to reduce clutter in the figure. The red vertical dashed line identifies the reference epoch. All cycles with good data coverage are shown. Dashed grey/black lines indicate the time interval when AT 2016blu was difficult to observe during each cycle. Black lines represent the evolution of AT 2016blu during 19 major outbursts. Quasi-periodic behaviour can be seen from the light curve of AT 2016blu, since peaks tend to occur near the red dashed line (or on either side of it when there are multiple peaks).

odogram and folded light curve, we showed that the variations are quasi-periodic. Similar to the case of SN 2000ch (Paper I), the quasi-periodic variability seen in the light curve has important implications for the cause of the outbursts. In the next section, we analyse *HST* observations to constrain the approximate initial mass and luminosity of AT 2016blu in its presumably quiescent state before the eruptive variability began. Next, in Section 7, we discuss an underlying mechanism that might trigger AT 2016blu's outbursts, and we note how this mechanism might account for both similarities and differences between AT 2016blu and SN 2000ch.

6 THE PROGENITOR

As mentioned in Section 3, past imaging from LOSS indicates no detection of eruptive variability in the period 1999–2009, despite frequent observations of the host galaxy. This implies that the progenitor star was not in an eruptive state prior to 2009 (or possibly prior to the first eruption detected in 2012). In that case, the *HST* images obtained in 2001 and 2005 allow us to constrain the properties of the relatively quiescent progenitor star.

6.1 Constraining the properties of the progenitor

Using *HST* observations described in Section 2.2, we built a spectral energy distribution (SED) from the extracted photometry in all of the bands, corrected for the assumed distance to the host galaxy NGC 4559 of 8.91 (±0.19 statistical, ±0.29 systematic) Mpc (McQuinn et al. 2017) and for foreground reddening. We show the resulting SED in Fig. 13. The uncertainties in the data points are driven mostly by the uncertainty in the distance.

The SEDs constructed from the 2001 and 2005 data tend to agree, implying that the star evolved little during that time period. The large excess in the *F*658*N* band indicates strong H α emission, which also affected the broad *F*606*W* band as well. Note that we assumed the host reddening to be small, equivalent to the foreground reddening, and did not apply any correction for possible circumstellar reddening (we return to this below), so values derived here are lower limits to the luminosity, temperature, and mass.

We then compared the photometry in the broad continuum bands from 2001 (*F*450*W*, *F*555*W*, and *F*814*W*) and 2005 (*F*435*W*, *F*555*W*, and *F*814*W*) to model SEDs from Binary Population and Spectral Synthesis (BPASS) v2.2.2 (Stanway & Eldridge 2018). The objective was to determine approximate values of effective temperature, $T_{\rm eff}$, and bolometric luminosity, $L_{\rm bol}$, matching the intrinsic colours of the progenitor. Over the range of BPASS single-star models [with zero-age main-sequence (ZAMS) masses $M_{\rm ZAMS} = 31$–35 M$_\odot$ for the 2001 data and a similar 32–37 M$_\odot$ for the 2005 data] that agreed with the colours, these corresponded to $T_{\rm eff} = 6745^{+302}_{-288}$ K and $\log(L_{\rm bol}/L_\odot) = 5.661^{+0.023}_{-0.031}$.

6.2 Temperature discrepancy and possible solutions

We note that a temperature of ∼7000 K is at odds with the He I line emission observed in the spectrum (see Section 2.4), which would normally indicate a much higher temperature $\gtrsim$20 000 K. Possible solutions to this discrepancy are that (1) AT 2016blu actually has a higher effective temperature of ∼20 000 K, but appears cooler in photometry because of reddening from additional circumstellar dust (this would also require a higher implied luminosity and initial mass than that derived above), (2) a hot companion star could assist in ionizing the wind or circumbinary material, or (3) shock excitation in wind collisions or colliding CSM shells could excite the He I. We defer this question to a future in-depth study of the spectral evolution of AT 2016blu; for now, we remain cognizant of the possibility that the temperature, luminosity, and implied initial mass are significantly higher than those derived from the *HST* SED, and we regard the values quoted above as lower limits.

Even without any correction for possible circumstellar dust, the lower limits on the mass and luminosity have important implications for AT 2016blu. Fig. 14 shows the estimated location of AT 2016blu's

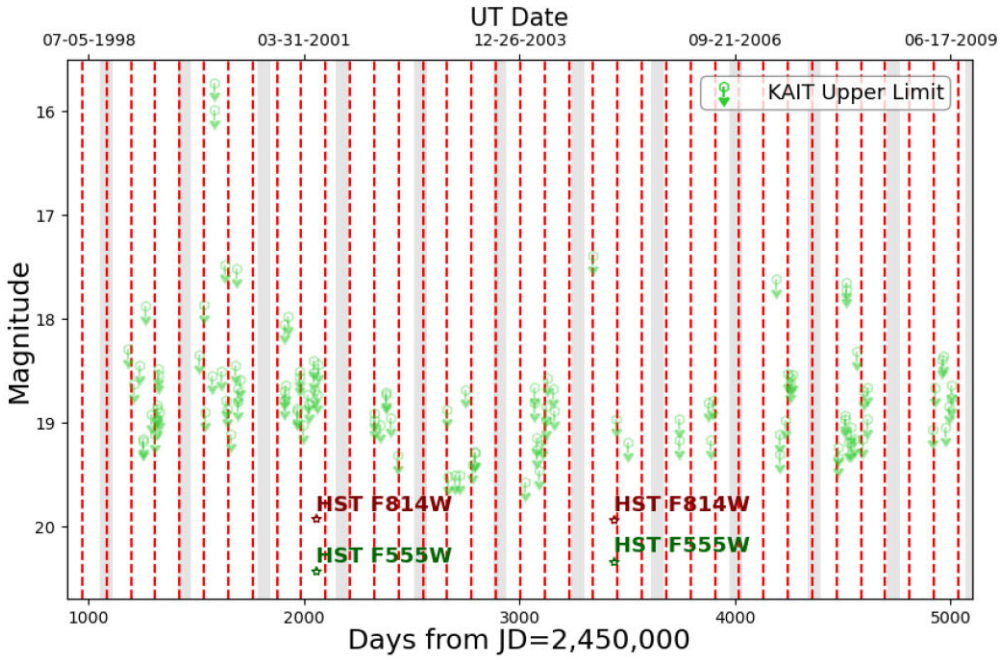

(a)

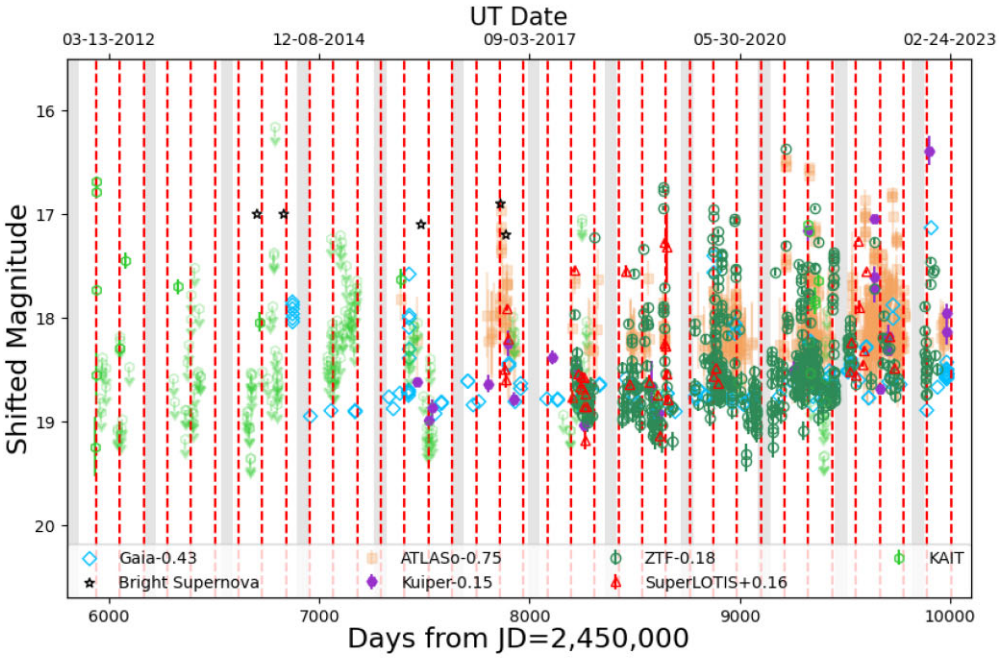

(b)

Figure 11. Same as Fig. 5, but with dashed red lines to indicate the reference epoch using a period of ∼113 d. The detected period matches with most of the outbursts, suggesting that the period is not changing much over time.

progenitor on the Hertzsprung–Russell (HR) diagram. The black circle notes the estimate corrected only for line-of-sight reddening. As noted above, this location was matched well by a BPASS model track for a single star with an initial mass of 33 $M_{\odot}$ (see Fig. 14). In this particular model, AT 2016blu would be on a blue loop, requiring that it would have had a much larger radius in a previous red supergiant phase. This might be problematic if it is in an interacting binary system, because that red supergiant would be much larger than the current orbit.

Alternatively, the position of the AT 2016blu's progenitor in the HR diagram can be roughly matched using a BPASS model designed for a single star with an initial mass of 37 $M_{\odot}$ (shown with an orange solid curve). In this model, the progenitor is still evolving across the HR diagram, approaching the red supergiant phase for the first time.

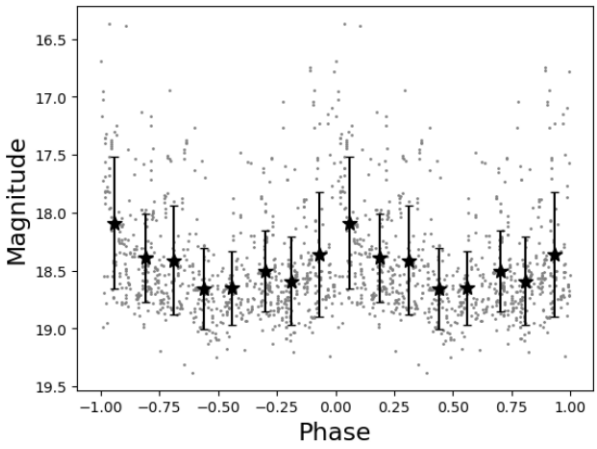

Figure 12. Phase diagram of AT 2016blu using the period of ∼113 d. Black points show average magnitudes after binning the folded light curve. AT 2016blu does tend to get brighter around phase zero.

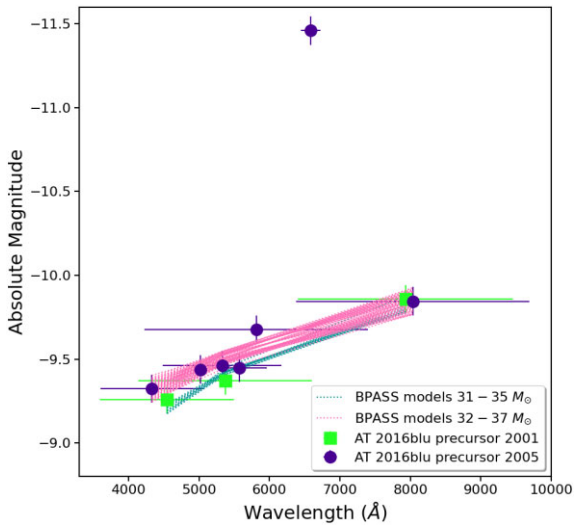

Figure 13. The SED of the AT 2016blu progenitor, established from the pre-outburst *HST* observations from 2001 and 2005 (see text). For comparison, we also show BPASS single-star model SEDs, with ZAMS masses ($M_{\rm ZAMS}$) as indicated in the legend.

Finally, the location of AT 2016blu's progenitor on the HR diagram can also be matched well with a BPASS model for an initially 40 $M_\odot$ primary star in a binary system (solid red curve in Fig. 14). However, in the next section, we discuss the reason why none of these models provides a satisfying explanation for the progenitor of AT 2016blu.

6.3 Comparison with LBVs and massive stars in the region

For comparison with AT 2016blu, Fig. 14 also shows LBVs and yellow hypergiants in the Milky Way and Local Group. We see that AT 2019blu lands amid the yellow hypergiants, although very close to LBVs in their cooler eruptive state indicated by the vertical grey bar. Any additional correction for circumstellar dust would move the star's position somewhere to its upper left, indicated by the blue ellipse, and thus would locate it amid the modulations experienced by the more luminous group of classical LBVs, making it too hot to be a yellow hypergiant. As noted earlier, the presence of He I emission in the spectrum gives reason to suspect that there may be

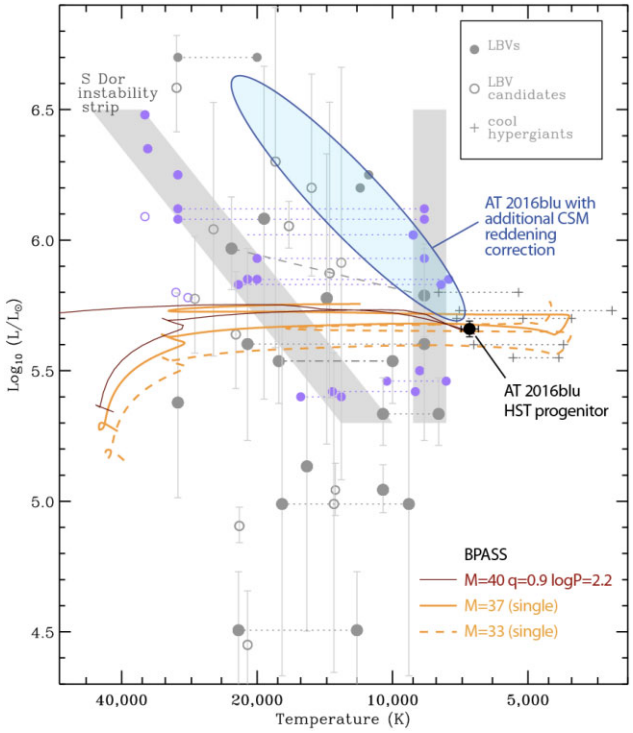

Figure 14. HR diagram showing the location of the 2001–2005 progenitor detected by *HST*, marked with a solid black circle. For comparison, we also show values for LBVs and LBV candidates in the Milky Way (grey circles) and in the Magellanic Clouds (violet circles) taken from Smith et al. (2019), as well as yellow hypergiants (grey 'plus signs') from Smith et al. 2004 (see those papers for additional details). Also for comparison, we plot BPASS stellar evolution models for a single star with $M_{\rm ZAMS} = 33$ $M_\odot$ (orange dashed track), $M_{\rm ZAMS} = 37$ $M_\odot$ (orange solid track), and a primary with $M_{\rm ZAMS} = 40$ $M_\odot$ in a binary with a mass ratio $q = 0.9$ and an orbital period of ∼150 d (dark red solid track). The blue ellipse shows an approximate range of locations for the progenitor of AT 2016blu if it were to be corrected for additional extinction from an unknown amount of CSM (the black point is only corrected for foreground ISM extinction). While we do not know the amount of CSM dust, additional reddening is motivated by the presence of He I emission, which likely requires $T_{\rm eff}$ significantly hotter than 7000 K (see text).

additional circumstellar reddening. No yellow hypergiant is known to show He I emission in its spectrum.

As previously mentioned, AT 2016blu stands out as the brightest star within the ∼175 pc radius shown in Fig. 1. There are several other blue and red supergiants in this region, which Soria et al. (2005) estimated to have initial masses of 10–15 $M_\odot$ and ages of ∼20 Myr, as noted earlier. If AT 2016blu's progenitor is interpreted as a single star with an initial mass of 33 $M_\odot$ (and therefore an age of around 5–6 Myr), then its age is incompatible with all the neighbouring massive stars. If it is a 40 $M_\odot$ primary star in a binary system (4–5 Myr), or if there is any additional circumstellar reddening, then this age discrepancy is even worse.

The progenitor of AT 2016blu was therefore clearly a massive blue straggler. This is something that the progenitor of AT 2016blu has in common with LBVs as well, with most LBVs being isolated from O-type stars (Smith & Tombleson 2015; Aghakhanloo et al. 2017). The rare LBVs that are found in clusters or associations with other massive stars, such as η Car, W243 in Wd1, R127, and S Dor, tend to stand out as far more luminous and often seem much younger than their siblings (Smith & Tombleson 2015; Smith 2016,

2019; Aghakhanloo et al. 2017, 2020; Beasor et al. 2021). Since AT 2016blu's progenitor was a massive blue straggler, it likely evolved as an interacting binary. As such, the BPASS model tracks included in Fig. 14 are probably not good representations of its past evolution, although they can match its current location on the HR diagram. (Even the binary BPASS track for a 40 $M_\odot$ primary shown in Fig. 14 is probably not applicable to AT 2016blu, since it is a mass donor in the system, with an age that is too young.) Instead, it is likely that the progenitor has evolved as a mass gainer in a binary or is the product of a stellar merger.

Given its location near LBVs on the HR diagram and its blue-straggler status that is shared by LBVs, we consider it likely that AT 2016blu's progenitor is indeed an LBV. This, combined with the quasi-periodicity of its eruptions, motivates a scenario wherein its repeating outbursts are caused by binary interaction, and where one of the stars in the system is an LBV, as discussed next.

7 LBV-MODULATED BINARY INTERACTION

The light-curve analysis of AT 2016blu shows periodic outbursts with irregular light curves, similar to those of SN 2000ch. In Paper I, we proposed that SN 2000ch's outbursts resemble photometric properties similar to the rapid brightening and fading observed in pre-SN eruptions of SN 2009ip (Smith et al. 2010; Pastorello et al. 2013), and η Car's periastron encounters leading to its Great Eruption (Smith 2011; Smith & Frew 2011). Therefore, we proposed that SN 2000ch's outbursts occur around times of periastron in an eccentric massive binary system, where the irregularity may arise because the interaction is modulated by erratic LBV-like instability in one of the two stars. The intrinsic variability of the LBV may not look the same as in normal LBVs because the interacting companion star can lead to mass-loss and hinder the expansion of the LBV, or because the intrinsic decade-long LBV brightness variations are mild compared to the more sudden and violent outbursts discussed here.

As we discussed in Section 3, similar to recent observations of SN 2000ch, AT 2016blu experienced an outburst every 3–4 months in the past decade. A regular periodicity of ∼113 d implies that there are two closely interacting stars, and a binary orbit governs the repeating events. AT 2016blu's light curve also exhibits a wide variety of peak luminosity, duration, and shape. Some events exhibit multiple rises and falls. As demonstrated in Section 3, the luminosity spikes occasionally occur before or after the anticipated time of outburst.

The quasi-periodic variability suggests that the binary orbit is eccentric (in other words, if the orbit were circular, then the level of interaction would be relatively constant and would not show outburst periodicity). When the separation between the two stars decreases at periastron, the interaction between the two stars – whatever the exact nature of that interaction may be – should be stronger.

The specific type of binary 'interaction' that is responsible for the brightening may arise from a variety of physical phenomena, including strong wind collisions (Pittard & Corcoran 2002; Okazaki et al. 2008; Kashi & Michaelis 2021), collision between the companion star and CSM (a shell or disc; Smith et al. 2018), grazing stellar collisions (Smith 2011), unsteady mass transfer and accretion (Soker 2004; Kashi & Soker 2009, 2010), etc. (this was discussed in detail in Paper I). A discussion of which of these may be responsible for the interaction in this case is postponed to a later time when we analyse spectra of AT 2016blu.

If the CSM is significantly clumpy or if accretion is unsteady, this could lead to multiple spikes in luminosity with approximately similar magnitudes that are clustered around times of periastron, but not exactly coincident with times of periastron. Multiple luminosity spikes may also be due to disconnected shells with cavities in between, perhaps analogous to the nested shells of dust around WR 140 that are created by repeated wind collisions (Lau et al. 2022). In this case, luminosity spikes might happen at different times relative to periastron, depending on the exact location of a dense shell. For example, if we presume that a brightness peak occurs when the companion encounters the densest CSM, and if circumstellar shells are thin, then the companion star may encounter the densest material somewhat before or after periastron. Averaged over many orbits, the brightness peaks would still tend to be clustered around times of periastron, even if they do not occur exactly at periastron.

As stated previously in Section 2, the *Gaia* baseline magnitude of AT 2016blu has increased by ∼0.5 mag over a period of ∼8 yr. For the luminosity and temperature derived from the progenitor's photometry (see Section 6), the corresponding radius is already near the maximum one would expect before strong interaction with a companion must start (i.e. the primary star's radius is comparable to the separation between the two stars). If the slow brightening of the baseline quiescent flux from *Gaia* indicates a continued expansion of the LBV star, then this expansion may trigger increasingly more violent interaction. Such expansion may also have initiated these eruptions a decade ago, with relatively weak or non-existent interaction before then.

In the binary scenario explained above, the companion star may be either a main-sequence star or an evolved star. If wind–wind interaction (i.e. colliding wind shocks) is the mechanism, both stars must be massive because the companion needs to have a strong wind. Alternatively, the companion star may be a compact object, in which case accretion on to a neutron star or black hole may be an interesting potential power source for AT 2016blu's eruptions. X-ray observations are needed to confirm the evidence of accretion on to a compact companion. Interestingly, in a blue straggler evolutionary scenario where AT 2016blu has evolved as a mass gainer (as discussed in the previous section), its companion – the initially more massive primary that was the mass donor – may have already exploded, perhaps leaving a compact object in an eccentric orbit.

The LBV-modulated binary interaction model proposed in our previous work has multiple free parameters such as orbital period, eccentricity, mass ratio, type of companion, etc. Physical parameters can vary in each system and can lead to very different light curves that may nevertheless share the common attribute of having quasi-periodic, irregular bright eruptions. For example, if AT 2016blu's orbit is somewhat less eccentric than that of SN 2000ch, then density fluctuations in the CSM (shells, discs) may cause the light curve to appear more irregular than that of SN 2000ch.

Using *HST* images, we have determined that AT 2016blu should have a mass and luminosity higher than $M \approx 33$ $M_\odot$ and $L \approx 10^{5.7}$ $L_\odot$ (see Section 6 for details). The photospheric radius of such a star is ∼38 $R_\odot$ (0.2 au) when it is in a hot quiescent state with an effective temperature of ∼25 000 K. However, if it is an LBV, then the photosphere should expand to ∼330 $R_\odot$ (1.5 au) during cooler outburst states with an effective temperature of ∼8500 K. Based on the observed orbital period of ∼113 d, the orbit's semimajor axis is estimated to be $a \approx 1.5\,\mathrm{au}\,(M_{\rm tot}/(M_{\rm primary} + M_{\rm secondary}))^{1/3}$. Here, $M_{\rm tot}$ represents the total mass of the system. However, as we do not currently have any information about the companion star, we assume it to be a star with a mass of 1 $M_\odot$. In other words, if the companion were a star with a mass of 10 $M_\odot$, the semimajor axis would be $a \approx 1.5\,\mathrm{au}\,(43M_{\rm tot}/34M_{\rm tot})^{1/3} \approx 1.6$ au. If the orbit of AT 2016blu is less eccentric compared to SN 2000ch with an eccentricity of ∼0.4, for instance, then the periastron separation would be about 0.9 au and the apastron distance ∼2.1 au.

At periastron, the distance between the two stars is smaller than the expanded radius of the LBV during its cooler eruptive state, which suggests a very strong interaction between the two stars. Conversely, at apastron, the distance between the stars is larger than the stellar radius, and interaction between the two stars may weaken or shut off. This could lead to cycles of interaction-driven outburst and quiescence. The intensity of the periastron interaction may also change slowly depending on the intrinsic state of the LBV. During some cycles, the interaction at periastron may be very weak, while at other times, we may expect more violent encounters as the LBV tries to expand.

As we mentioned above, the LBV in its outburst state is expected to have a radius of 1.5 au, while the predicted periastron distance is only ∼0.9 au. In such a scenario, it may be possible for a companion star to briefly enter the LBV's stellar envelope, but it may not necessarily lead to the merging of the two stars owing to the small amount of mass contained within the outer envelope. However, a merger may eventually be triggered by the friction in these repeated encounters, so continued monitoring of AT 2016blu is worthwhile. So far, we do not see strong evidence that the orbital period is changing.

There may be other mechanisms, beyond what we have proposed, that could account for the observed outbursts and periodicity of AT 2016blu without the need to invoke binarity. One alternative scenario might be that the behaviour is caused by an instability within a single massive star. Currently, however, we are aware of no predictions from single-star models that can account for quasi-periodic outbursts with a rapid and substantial change in luminosity comparable to those seen in AT 2016blu or SN 2000ch.

8 SUMMARY AND CONCLUSION

We present the first analysis of photometric observations of AT 2016blu (=NGC 4559OT). AT 2016blu experienced its first known outburst in 2012 January. Since that time, optical observations reveal that AT 2016blu experienced at least 19 known outbursts in 2012–2022. Two of these outbursts in 2014 and 2016 are also detected in the IR by *Spitzer*. The outburst light curves show a wide variety of shapes, durations, and amplitudes. While the outbursts are irregular and multipeaked, our investigation demonstrates that they do repeat with a period of ∼113 ± 2 d.

We propose that AT 2016blu's outbursts are driven by interaction between two stars at periastron in an eccentric binary system, where the primary star is a massive LBV and the companion star may be a compact object or another star. Using *HST* observations, we find that the mass and luminosity of AT 2016blu should be higher than $M \approx 33\ M_\odot$ and $L \approx 10^{5.7}\ L_\odot$, respectively. These may be larger if there is circumstellar extinction that we have not taken into account.

In a binary interaction scenario, the strength of periastron interaction between two stars may vary depending on the state of the LBV around the time of the periastron passage. An interaction with the companion at periastron may be relatively weak when the LBV is in a quiescent state with small stellar radius and low mass-loss rate. Stronger interactions are expected, however, in periastron passes when the LBV has an inflated radius during an S Dor excursion and perhaps a higher mass-loss rate. Thus, successive periastron eruptions may look different each time.

The proposed binary interaction of AT 2016blu is similar to the periastron encounters envisioned for SN 2000ch (Paper I), SN 2009ip (Pastorello et al. 2013; Smith & Arnett 2014; Smith et al. 2022), and η Car (Smith 2011; Smith et al. 2018). The outbursts of AT 2016blu are less regular and less periodic than those of SN 2000ch, indicating that the AT 2016blu system may have a less eccentric orbit with significantly clumpy CSM, multiple expanding dust shells, or unsteady accretion on to the compact companion. Further studies are required to understand the nature of the companion and underlying physics causing multiple spikes in the light curve.

SN 2000ch and AT 2016blu are so far the only studied extragalactic LBVs that exhibit quasi-periodic behaviour in their major outburst variability. According to some studies in the literature, AG Car in the Milky Way, as well as Large Magellanic Cloud LBV S Dor, exhibits quasi-periodic behaviour, and η Car is an eccentric colliding-wind binary with a period of 5.5 yr (van Genderen, Sterken & de Groot 1997; Damineli et al. 2008). However, these estimated periods are longer than those of AT 2016blu and SN 2000ch, and are associated with the small-amplitude variability of LBVs, or (in the case of η Car) colliding winds that have little impact on the total luminosity.

Given the detected period of ∼113 d, we predict that AT 2016blu's next outburst will be around late 2023 February/March[5] and then again in late 2023 June, 2023 October, and 2024 February, although the event in 2023 October is likely to be unobservable. Since AT 2016blu's light curve shows that the outbursts are usually brief, multipeaked, and sometimes occur before or after the expected time of periastron, it would be worthwhile to monitor AT 2016blu with high-cadence photometry and spectroscopy for about a month before and after the proposed timelines. We encourage further monitoring and detailed observations of AT 2016blu considering that it may be a prelude to a merger or SN explosion, similar to SN 2009ip.

ACKNOWLEDGEMENTS

We thank the anonymous referee for helpful comments that improved the quality of this paper. This research has made use of the NASA/IPAC Infrared Science Archive, which is funded by the National Aeronautics and Space Administration (NASA) and operated by the California Institute of Technology. It also used data from the ATLAS project, which is funded primarily to search for near-Earth objects (NEOs) through NASA grants NN12AR55G, 80NSSC18K0284, and 80NSSC18K1575; by-products of the NEO search include images and catalogues from the survey area. The ATLAS science products have been made possible through the contributions of the University of Hawaii Institute for Astronomy, the Queen's University Belfast, the Space Telescope Science Institute (STScI), the South African Astronomical Observatory, and the Millennium Institute of Astrophysics (MAS), Chile. We also acknowledge ESA *Gaia*, DPAC, and the Photometric Science Alerts Team (http://gsaweb.ast.cam.ac.uk/alerts). This work is also based on observations made with the *Spitzer*, which is operated by the Jet Propulsion Laboratory, California Institute of Technology, under a contract with NASA.

This work was partially funded by Kepler/K2 grant J1944/80NSSC19K0112, as well as by STFC grants ST/T000198/1 and ST/S006109/1. Financial support was provided by NASA through *HST* grants AR-14259, AR-14316, and GO-15889 from STScI, which is operated by the Association of Universities for Research in Astronomy (AURA), Inc., under NASA contract NAS5-26555. AVF's group at UC Berkeley has received generous financial assistance from the Christopher R. Redlich Fund, Alan Eustace (WZ is a Eustace Specialist in Astronomy), and numerous individual donors. KAIT and its ongoing operation were made possible by

[5]This date is before the publication date, but well after the original submission date. At the time of resubmitting this paper, we do not analyse data covering this event.

donations from Sun Microsystems, Inc., the Hewlett-Packard Company, AutoScope Corporation, Lick Observatory, the U.S. National Science Foundation (NSF), the University of California, the Sylvia & Jim Katzman Foundation, and the TABASGO Foundation. Research at Lick Observatory is partially supported by a generous gift from Google. JEA was supported by the international Gemini Observatory, a programme of NSF's NOIRLab, which is managed by AURA, Inc., under a cooperative agreement with the NSF, on behalf of the Gemini partnership of Argentina, Brazil, Canada, Chile, the Republic of Korea, and the USA.

DATA AVAILABILITY

The KAIT, Super-LOTIS, Kuiper, and *Spitzer* data used in this work are available in the article. ZTF data are available in the public domain (https://irsa.ipac.caltech.edu/Missions/ztf.html). ATLAS data are available in the ATLAS Forced Photometry server (https://fallingstar-data.com/forcedphot/). *Gaia* data are available at http://gsaweb.ast.cam.ac.uk/alerts/home. The 'Bright Supernovae' data are available at https://www.rochesterastronomy.org/supernova.html.

REFERENCES

Aghakhanloo M., Murphy J. W., Smith N., Hložek R., 2017, MNRAS, 472, 591
Aghakhanloo M. et al., 2020, MNRAS, 492, 2497
Aghakhanloo M. et al., 2023, MNRAS, 521, 1941(Paper I)
Arbour R., 2016, Transient Name Server Discovery Report, No. 2016-266
Beasor E. R., Davies B., Smith N., Gehrz R. D., Figer D. F., 2021, ApJ, 912, 16
Bellm E. C. et al., 2019, PASP, 131, 068003
Bonanos A. Z. et al., 2010, AJ, 140, 416
Brennan S. J., Elias-Rosa N., Fraser M., Van Dyk S. D., Lyman J. D., 2022, A&A, 664, L18
Damineli A. et al., 2008, MNRAS, 384, 1649
Dolphin A., 2016, Astrophysics Source Code Library, record ascl:1608.013
Filippenko A. V., Li W. D., Treffers R. R., Modjaz M., 2001, in Paczynski B., Chen W.-P., Lemme C., eds, ASP Conf. Ser. Vol. 246, IAU Colloq. 183: Small Telescope Astronomy on Global Scales. Astron. Soc. Pac., San Francisco, p. 121
Gaia Collaboration, 2016, A&A, 595, A1
Hodgkin S. T. et al., 2021, A&A, 652, A76
Jencson J. E., Sand D. J., Andrews J. E., Smith N., Strader J., Aghakhanloo M., Pearson J., Valenti S., 2022, ApJ, 935, L33
Kandrashoff M. et al., 2012, Cent. Bur. Electron. Telegrams, 2976, 1
Kashi A., Michaelis A., 2021, Galaxies, 10, 4
Kashi A., Soker N., 2009, New Astron., 14, 11
Kashi A., Soker N., 2010, ApJ, 723, 602
Lau R. M. et al., 2022, Nat. Astron., 6, 1308
Law N. M. et al., 2009, PASP, 121, 1395
Li W. D. et al., 2000, in Holt S. S., Zhang W. W., eds, AIP Conf. Proc. Vol. 522, Cosmic Explosions: Tenth Astrophysics Conference. Am. Inst. Phys., New York, p. 103
Li W., Filippenko A. V., Chornock R., Jha S., 2003, ApJ, 586, L9
Lomb N. R., 1976, Ap&SS, 39, 447
Mauerhan J. C. et al., 2013, MNRAS, 430, 1801
McQuinn K. B. W., Skillman E. D., Dolphin A. E., Berg D., Kennicutt R., 2017, AJ, 154, 51
Okazaki A. T., Owocki S. P., Russell C. M. P., Corcoran M. F., 2008, MNRAS, 388, L39
Pastorello A. et al., 2010, MNRAS, 408, 181
Pastorello A. et al., 2013, ApJ, 767, 1
Pittard J. M., Corcoran M. F., 2002, A&A, 383, 636
Scargle J. D., 1982, ApJ, 263, 835
Schlafly E. F., Finkbeiner D. P., 2011, ApJ, 737, 103
Sheehan P. et al., 2014, Astron. Telegram, 6303, 1
Smith N., 2011, MNRAS, 415, 2020
Smith N., 2016, MNRAS, 461, 3353
Smith N., 2019, MNRAS, 489, 4378
Smith N., Arnett W. D., 2014, ApJ, 785, 82
Smith N., Frew D. J., 2011, MNRAS, 415, 2009
Smith N., Tombleson R., 2015, MNRAS, 447, 598
Smith N. et al., 2010, AJ, 139, 1451
Smith N., Li W., Silverman J. M., Ganeshalingam M., Filippenko A. V., 2011, MNRAS, 415, 773
Smith N. et al., 2018, MNRAS, 480, 1466
Smith N., Aghakhanloo M., Murphy J. W., Drout M. R., Stassun K. G., Groh J. H., 2019, MNRAS, 488, 1760
Smith N. et al., 2020, MNRAS, 492, 5897
Smith N., Andrews J. E., Filippenko A. V., Fox O. D., Mauerhan J. C., Van Dyk S. D., 2022, MNRAS, 515, 71
Soker N., 2004, ApJ, 612, 1060
Soria R., Cropper M., Pakull M., Mushotzky R., Wu K., 2005, MNRAS, 356, 12
Stanway E. R., Eldridge J. J., 2018, MNRAS, 479, 75
STSCI Development Team, 2012, Astrophysics Source Code Library, record ascl:1212.011
Tonry J. L. et al., 2018, PASP, 130, 064505
Van Dyk S. D., Peng C. Y., King J. Y., Filippenko A. V., Treffers R. R., Li W., Richmond M. W., 2000, PASP, 112, 1532
Van Dyk S. D., Ganeshalingam M., Silverman J. M., Filippenko A. V., 2012, Astron. Telegram, 3865, 1
van Genderen A. M., Sterken C., de Groot M., 1997, A&A, 318, 81
VanderPlas J. T., 2018, ApJS, 236, 16
Wagner R. M. et al., 2004, PASP, 116, 326
Williams G. G., Milne P. A., Park H. S., Barthelmy S. D., Hartmann D. H., Updike A., Hurley K., 2008, in Galassi M., Palmer D., Fenimore E., eds, AIP Conf. Proc. Vol. 1000, Gamma-ray Bursts 2007: Proceedings of the Santa Fe Conference. Am. Inst. Phys., New York, p. 535

SUPPORTING INFORMATION

Supplementary data are available at *MNRAS* online.

suppl_data

Please note: Oxford University Press is not responsible for the content or functionality of any supporting materials supplied by the authors. Any queries (other than missing material) should be directed to the corresponding author for the article.

APPENDIX A: THE PHOTOMETRIC DATA

The photometric data used in this work are presented in the following tables. All photometric data presented below are in the Vega system.

Table A1. Unfiltered KAIT photometry (∼*R* band).

JD	Mag	σ
2455 936.04	19.24	0.28
2455 938.04	16.78	0.04
2455 938.91	16.69	0.04
2455 940.05	17.73	0.07
2455 942.03	18.55	0.28
2456 048.77	18.30	0.12
2456 076.74	17.45	0.08
2456 327.88	17.70	0.08
2456 713.93	18.04	0.09
2457 387.08	17.62	0.10
2459 371.74	17.64	0.06
2459 357.81	17.86	0.11
2459 358.81	17.83	0.12
2459 324.90	17.10	0.04
2459 326.89	17.17	0.06

Table A2. Super-LOTIS photometry.

JD	R	σ_R	V	σ_V	I	σ_I
2457 879.80	18.35	0.06	18.35	0.05		
2457 885.80	18.45	0.07	18.32	0.07		
2457 893.80	17.82	0.02	17.94	0.02		
2457 895.80	18.09	0.05	18.19	0.05		
2458 204.90	18.59	0.07			16.61	0.41
2458 213.90	17.48	0.03			17.68	0.04
2458 229.90	18.39	0.04			18.87	0.06
2458 242.80	18.51	0.04				
2458 246.80	18.42	0.04				
2458 255.80	18.52	0.04				
2458 257.80	18.67	0.04				
2458 258.80	18.42	0.04				
2458 263.60	18.56	0.04				
2458 266.60	18.93	0.09				
2458 269.60	18.66	0.06				
2458 457.00	17.49	0.06	17.41	0.05		
2458 473.00	18.48	0.10	18.76	0.09		
2458 567.00	18.47	0.07				
2458 606.80	18.57	0.05	18.57	0.04		
2458 618.80	18.89	0.11				
2458 638.80	17.22	0.03				
2458 640.80	18.14	0.04				
2458 645.70	18.15	0.09				
2458 651.80	17.27	0.34				
2458 654.70	18.40	0.05				
2458 660.70	18.61	0.04				
2458 871.90	18.41	0.02				
2458 886.90	18.35	0.03				
2458 894.90	18.47	0.02				
2459 525.00	18.38	0.04				
2459 531.00	18.12	0.03				
2459 554.00	18.40	0.02				
2459 560.00	17.21	0.01				
2459 566.00	17.81	0.06				
2459 586.00	18.32	0.02				
2459 592.00	18.19	0.03				
2459 601.00	17.49	0.02				
2459 710.80	18.08	0.04	18.01	0.04		
2459 733.70	18.34	0.03	18.59	0.03		

Table A3. Kuiper/MONT4K photometry.

JD	Harris-R	σ_R
2457 466.77	18.82	0.05
2457 520.81	19.28	0.06
2457 535.79	19.13	0.08
2457 805.88	18.84	0.08
2457 900.80	18.39	0.12
2457 923.77	19.03	0.07
2458 108.92	18.54	0.07
2458 227.79	18.73	0.15
2458 257.83	19.35	0.07
2458 582.78	18.87	0.24
2458 612.80	19.19	0.14
2459 257.82	18.69	0.09
2459 321.85	18.49	0.02
2459 322.83	17.20	0.13
2459 345.88	18.45	0.11
2459 639.98	17.09	0.02
2459 640.90	17.68	0.10
2459 641.80	17.80	0.14
2459 666.76	18.91	0.05
2459 706.79	18.46	0.03
2459 707.82	18.31	0.12
2459 903.01	16.41	0.14
2459 984.78	18.26	0.12
2459 985.82	18.06	0.09

Table A4. *HST* raw photometry.

JD	*HST* mode	Spectral element	Mag	σ
2452 054.5	WFPC2	*F*450*W*	20.552	0.006
		*F*555*W*	20.427	0.005
		*F*814*W*	19.920	0.005
2453 437.5	ACS/HRC	*F*435*W*	20.489	0.003
		*F*555*W*	20.336	0.003
		*F*814*W*	19.932	0.003

Table A5. *Spitzer*/IRAC photometry.

JD	$\text{Mag}_{[3.6]}$	$\sigma_{[3.6]}$	$\text{Mag}_{[4.5]}$	$\sigma_{[4.5]}$	Colour[a]
2453 148.87	17.05	0.06	16.90	0.08	–
2453 152.21	17.13	0.07	16.91	0.09	–
2456 723.28	16.66	0.04	16.34	0.04	0.49
2456 751.17	16.98	0.05	16.74	0.06	0.43
2456 906.66	17.04	0.05	16.83	0.07	0.14
2457 092.01	17.09	0.05	16.84	0.06	1.06
2457 251.25	16.92	0.05	16.56	0.04	0.92
2457 466.48	16.88	0.05	16.60	0.05	0.51
2457 472.39	16.63	0.04	16.28	0.03	0.55
2457 487.16	16.86	0.04	16.45	0.04	0.89
2457 619.52	17.08	0.06	16.76	0.05	1.63
2457 627.15	17.13	0.06	16.91	0.07	–
2457 648.27	17.10	0.05	16.89	0.06	0.17

[a]After subtracting the minimum observed flux before 2012.

This paper has been typeset from a TEX/LATEX file prepared by the author.